



## Electron cyclotron heating experiments on the JFT-2 tokamak using an inside launch antenna

C. P. Moeller, V. S. Chan, R. J. La Haye, R. Prater, T. Yamamoto, A. Funahashi, K. Hoshino, and T. Yamouchi

Citation: [Physics of Fluids](#) **25**, 1211 (1982); doi: 10.1063/1.863892

View online: <http://dx.doi.org/10.1063/1.863892>

View Table of Contents: <http://scitation.aip.org/content/aip/journal/pof1/25/7?ver=pdfcov>

Published by the [AIP Publishing](#)

---

### Articles you may be interested in

[Electron Cyclotron / Bernstein Wave Heating and Current Drive Experiments using Phased-array Antenna in QUEST](#)

AIP Conf. Proc. **1406**, 473 (2011); 10.1063/1.3665017

[Suppression of  \$m=2\$  islands by electron cyclotron heating in the Texas Experimental Tokamak: Experiment and theory](#)

Phys. Fluids B **5**, 3239 (1993); 10.1063/1.860659

[IBW experiment on JFT-2M tokamak](#)

AIP Conf. Proc. **190**, 350 (1989); 10.1063/1.38469

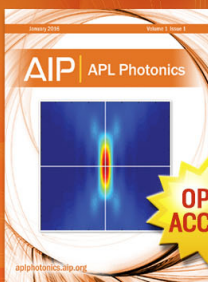
[Electron cyclotron current drive and heating experiments on the WT-3 tokamak](#)

AIP Conf. Proc. **190**, 88 (1989); 10.1063/1.38465

[Discharge cleaning experiment in the JFT-2 tokamak with surface observation by AES](#)

J. Vac. Sci. Technol. **15**, 103 (1978); 10.1116/1.569414

---



Launching in 2016!  
The future of applied photonics research is here

OPEN  
ACCESS

AIP | APL  
Photonics

# Electron cyclotron heating experiments on the JFT-2 tokamak using an inside launch antenna

C. P. Moeller, V. S. Chan, R. J. La Haye, and R. Prater  
*General Atomic Company, San Diego, California 92138*

T. Yamamoto, A. Funahashi, K. Hoshino, T. Yamouchi  
*Japan Atomic Energy Research Institute, Tokai, Japan*

(Received 8 September 1981; accepted 8 April 1982)

An electron cyclotron heating experiment is described in which 28 GHz microwave power is launched from the high field side (inside) of a tokamak discharge from a steerable phased array antenna exciting the extraordinary mode. The central temperature was doubled (from 600 eV to 1200 eV) with a power at the antenna approximately two-thirds the Ohmic input. An oblique launch of the extraordinary mode was found to heat more efficiently and to a higher density than either the perpendicularly launched extraordinary mode or the ordinary mode launched from the outside.

## I. INTRODUCTION

The principal objective of the electron cyclotron heating experiments on the JFT-2 tokamak was to launch relatively pure modes (ordinary or extraordinary) at well-defined launch angles in order to compare their heating efficiencies, the predicted damping and heating efficiency depending strongly on the mode and launch angle. Since the development of gyrotrons capable of millisecond or longer pulse lengths, electron cyclotron heating experiments have been performed on many tokamaks, but for only two of these, the T-10 and FT-1<sup>1</sup> machines, have results been reported in which the polarization of the incident microwave power was controlled, and only the latter experiment was at the fundamental resonance. The FT-1 experiment claimed a very significant improvement in the density limit of heating for an inside launch, but the initial electron temperature, approximately 100 eV, and the relatively small increases, approximately 20 eV, did not permit a true test of the damping processes that are important at higher temperatures.

For the experiments performed on the JFT-2 tokamak, on the other hand, the initial electron temperature was 600 eV, which puts it well into the regime where the high-temperature direct damping processes are important.

The outside launch electron cyclotron heating experiments on JFT-2 have been described elsewhere.<sup>2</sup> For the inside launch experiments to be described here, there are three theoretically predicted damping mechanisms expected, depending on the polarization and launch angle at the antenna. For the extraordinary mode there are two competing mechanisms, namely, direct damping at the cyclotron resonance surface<sup>3-6</sup> and mode conversion near the upper hybrid layer.<sup>7,8</sup> The first mechanism is only important at relatively high temperatures ( $\gtrsim 500$  eV) and for an oblique launch angle, while the second will be present for any launch angle and finite temperature. The ordinary mode may also be launched from inside and be damped by the direct cyclotron damping process, but it is equally accessible from the outside, so we have not examined it here.

The inverse of the mode conversion heating process, on

which the fundamental resonance cyclotron radiometer relies, has been demonstrated to work in tokamak discharges.<sup>9</sup> Since this damping process is predicted to be effective for a perpendicular launch, it would appear to be the most attractive approach, insofar as there would be an improvement of a full factor of two in cutoff density compared with that for the ordinary mode. However, since the mode conversion approach depends on a slow electrostatic wave (the electron Bernstein wave) carrying high power from near the outside (low field) plasma edge to the cyclotron resonant surface, there is the possibility of nonlinear damping near the plasma edge.<sup>10,11</sup>

The direct cyclotron damping process, because an oblique launch angle is required to obtain strong damping, will have a density cutoff for our parameter range of  $2(1 - n_{\parallel}^2)n_c$  (Ref. 6), where  $n_{\parallel}$  is the local parallel index of refraction and  $n_c$  is the ordinary mode cutoff density. Even in JFT-2, very strong damping can be expected with a central  $n_{\parallel} = 0.44$  giving a cutoff of  $1.6n_c$ , while in higher temperature tokamaks,  $n_{\parallel}$  could be considerably smaller. This slight decrease in cutoff density is also mitigated by the fact that for profile heating, the extraordinary wave need penetrate only to the resonant surface, unlike the mode conversion process, which requires propagation across almost the full minor diameter of the discharge.

Of course, wave energy undamped by the direct process will travel to the upper hybrid layer where mode conversion can occur, so that it might appear difficult to separate the effects in the case of an oblique launch. In fact, as will be seen from the data to be presented, the heating ascribable to the mode conversion process becomes very poor at higher density, so that the effects are quite separable.

## II. MICROWAVE SYSTEM AND TOKAMAK CHARACTERISTICS

The JFT-2 tokamak has a major radius of 90 cm and a minor chamber radius of 31 cm, with the main limiter normally set at 25 cm. When operated with a toroidal field of 1 T and a plasma current of 75 kA (the current was limited to

prevent excessive runaway electron generation at the low densities required for this experiment), the electron temperature was approximately 600 eV, while the one turn voltage was typically 1.2–1.5 V.

The available diagnostics most relevant to electron heating are a scanable Thomson scattering system, a wide angle soft x-ray pulse height analysis system, a second harmonic radiometer, and a soft x-ray pin diode array. Although the latter two diagnostics provided some interesting qualitative information, their signals often showed increases with heating far too large to be indicative of a meaningful temperature, so that the data presented here are only from the first two diagnostics listed. The latter two diagnostics have the disadvantage that they can respond to small numbers of high-energy electrons, and unlike the first two diagnostics, the contribution from different parts of the distribution function is not available in the raw data.

A simplified schematic of the microwave system is shown in Fig. 1. The gyrotron delivers 200 kW at 28 GHz, primarily in the  $TE_{02}$  circular electric mode in 6.35 cm diam. waveguide. That mode is not itself useful for exciting a pure mode in the plasma, so that at some point in the system it is necessary to convert to a linearly or elliptically polarized field.

Although there are quasi-optical techniques for accomplishing this (such as mode converting antennas), at 28 GHz they would have been far too big for use inside the JFT-2 tokamak. Instead, we chose to immediately convert to the  $TE_{10}$  fundamental rectangular waveguide mode, the use of which is still feasible at 28 GHz. This conversion is accomplished by what is essentially a generalized directional coupler,<sup>12</sup> its input arm being the 6.35 cm circular guide and its output “arm” consisting of eight rectangular waveguides which are each coupled by a long slot in their narrow wall to the circular guide. Any power unconverted is absorbed in a high-power load attached to the opposite end of the circular guide. In low-power tests using a  $TE_{02}$  mode source of high purity, an efficiency close to 90% was measured, with the output powers equal to within 5%. When connected to the gyrotron with the power supply parameters set to give 200 kW directly into a matched load, we measured  $21 \pm 1$  kW per arm into a small water load, giving an efficiency exceed-

ing 80%, with another 30 kW appearing in the load terminating the circular guide.

By converting to standard rectangular waveguide (inside dimensions  $1.067 \text{ cm} \times 0.432 \text{ cm}$ ) it is then possible to use commercially available components such as directional couplers and loads and, of greater importance, the antenna technology developed for radar.

As indicated in Fig. 1, for each of the eight lines there is a directional coupler for waveguide arc detection and power monitoring, followed by a run of approximately 2 m to the JFT-2 vacuum vessel. At the vessel, each of the lines is connected to a calibrated phase shifter mounted on the vacuum flange. The rectangular waveguides, with their interiors still at atmospheric pressure, continue down around the inside wall of the vacuum vessel to the waveguide vacuum windows, which are located well beyond the cyclotron resonance layer in order to avoid resonant breakdown in the waveguides.

Located a few centimeters beyond the windows is the slotted waveguide phased array antenna, a photograph of which is shown in Fig. 2. With such a phased array, the beam pattern can be steered in the toroidal direction by an adjustment of the external phase shifters, without requiring any moving parts inside the vacuum vessel. The array consists of a row of eight parallel rectangular waveguides (machined from a split copper block) with adjacent pairs of guides sharing a common broad wall and with their axes perpendicular to the toroidal field. The slots in each guide, which are in the narrow wall and spaced one guide wavelength apart, form a vertical broadside resonant array, while each guide is an element of the steerable horizontal array.<sup>13</sup>

To launch, exclusively, the extraordinary mode at an oblique angle, an elliptically polarized field is required at the plasma edge,<sup>5</sup> the ratio of horizontally to vertically polarized electric field components being

$$|E_H/E_V| = (\omega_c/\omega) \{ - (1 - n_{\parallel}^2) + [(1 - n_{\parallel}^2)^2 + 4n_{\parallel}^2\omega^2/\omega_c^2]^{1/2} \} / 2n_{\parallel}, \quad (1)$$

where  $\omega_c$  is the value of the electron cyclotron resonant angular frequency at the antenna and  $n_{\parallel} = k_{\parallel}c/\omega$ ,  $k_{\parallel}$  is the wavenumber imposed by the antenna in the direction of the

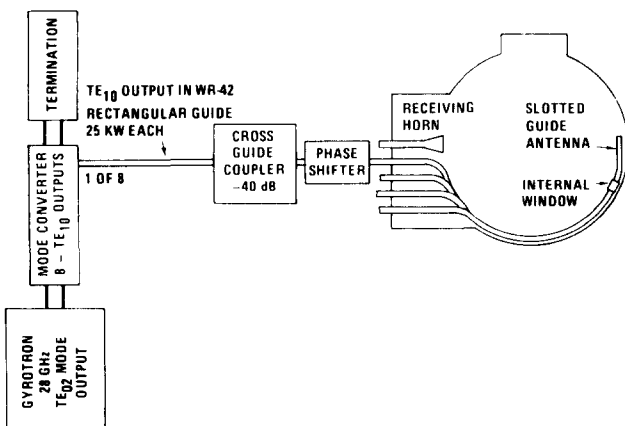


FIG. 1. Schematic diagram of the microwave system.

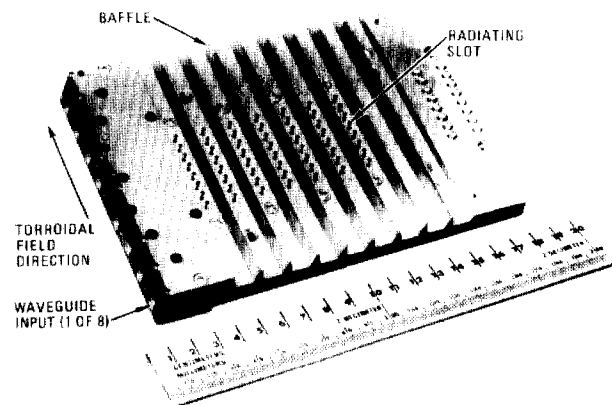


FIG. 2. Photograph of the slotted waveguide, phased array antenna.

magnetic field,  $c$  is the velocity of light, and  $\omega$  is the applied angular frequency. This result is obtained by using the low-density limit of the cold plasma dispersion relation to solve for the field components.<sup>14</sup>

The elliptically polarized field is obtained by a combination of the slanted slots and the horizontal baffles indicated in Fig. 2. The slots produce both a horizontal and vertical component of electric field, the phase of the horizontally polarized component being delayed approximately  $90^\circ$  more than the vertical component as they propagate through the horizontal baffles. The measured ratio of horizontal to vertical electric field is such that in the range  $0.66 < n_{\parallel} < 0.86$  ( $42^\circ$ – $60^\circ$  to the perpendicular in the direction of the toroidal field) primarily the extraordinary mode is excited, while for perpendicular propagation the division of power should be 75% to the extraordinary mode and 25% to the ordinary mode.

The initial equalization of the phases of the eight lines was made after the installation of the system by adjusting the phase shifters in pairs to maximize the signal at the receiving horn facing the antenna, the adjustment being done without plasma. In spite of the fact that the measurement was made in a metallic vacuum vessel, the maximum was very clear and the reflected power very small, possibly because the many ports on the vessel greatly reduce its  $Q$ . Once the phase settings for perpendicular propagation were obtained, any other launch angle could be obtained by appropriately adjusting the calibrated phase shifters. The beam width measured by sweeping the beam pattern past the receiving horn is  $8^\circ$  half-angle at half-maximum.

Dividing the 160 kW among eight circuits kept the electric fields to manageable, although not really conservative, levels. The highest electric field in the rectangular guide was 9 kV/cm, while the peak field at the 1 cm diameter ceramic windows was 5 kV/cm. With the waveguides filled with dry nitrogen at atmospheric pressure, seven of the eight circuits performed quite reliably, while the remaining one had sufficiently frequent arcs at an inaccessible location that we chose to terminate it near the mode converter in a high-power load in order to obtain experimental data at a reasonable rate. Fortunately the offending circuit fed an outside element of the antenna, so terminating it did not seriously degrade the antenna pattern.

The maximum power available at the antenna was also reduced by the waveguide losses, which for the approximately 3 m run were measured to be 30%. The mode converter and waveguide losses combined reduced the available power to 116 kW, 7/8 of that being 101 kW. In actual operation with the antenna, the gyrotron put out no more than 170 kW according to a water load measurement made using the terminated arm, so that we typically operated with no more than 85 kW at the antenna. Although the overall efficiency of the microwave system would hardly be acceptable for bulk heating of a large tokamak, it did provide the control of polarization and launch angle required for the purposes of this experiment within the constraints imposed by the wavelength and vacuum vessel. In a larger tokamak and/or at shorter wavelengths, a pure mode could be excited at a well-defined launch angle with high overall efficiency using direct

transmission of a circular electric mode and a quasi-optical antenna.

### III. EXPERIMENTAL RESULTS

There are several preliminary remarks to be made about the data.

The rf pulse was normally applied 60 msec into the discharge, while the Thomson scattering measurement was made 10 msec into the 15 msec long pulse. The soft x-ray data points represent an accumulation of counts in 5 msec long blocks, with the presented data points being from the 65 to 70 msec blocks. Typically, 30 good shots were needed to obtain a soft x-ray data point, while photon counts from several shots were averaged to improve the Thomson scattering statistics.

As will be seen, the soft x-ray temperatures during heating are consistently higher than the Thomson scattering values. This is also true to a lesser extent with just the Ohmic discharge. In neither case is there normally evidence of a true tail, i.e., a two-component distribution at the soft x-ray energies, so that if the distribution is non-Maxwellian the break occurs in the range 1 to 2 keV, outside the range of either diagnostic.

The central densities at which we operated were rather marginal for the Thomson scattering system, so that an accumulation of counts from several shots was needed to obtain acceptable statistics. The lower densities and temperatures away from the center made temperature profile measurements very marginal indeed, with the consequence that we have no temperature profile data.

The data to be presented are in the form of central temperature as a function of density for various launch angles and magnetic fields. This form was chosen because the density reduction that occurs during heating, which can be as great as 40% of the initial value, depends on all three parameters, so that the density cannot readily be held constant during a scan. The cause of this density reduction, which has been seen in previous electron cyclotron heating experiments,<sup>2,15</sup> may be associated with edge heating, but is not well-understood.

The central density scale used in Figs. 3 through 7 is obtained from the measured line average density during the rf pulse by multiplying the line average value by the factor 1.7, which is approximately the peak to average ratio in the absence of heating. The scale factor is merely intended to facilitate comparison of the data with theory. In those cases where sufficient density data were available from Thomson scattering, the fractional reduction in density indicated by the Thomson scattering was within  $\pm 20\%$  of the fractional reduction of the line average value. We could not use the in-principle absolute density data provided by the Thomson scattering because the system was not kept in calibration by Rayleigh scattering.

One predicted feature of the extraordinary mode propagation was immediately verified using the receiving horn facing the antenna, namely that the extraordinary mode cannot propagate through the upper hybrid layer even at high power. With the array phased for perpendicular propagation, the plasma, even at a density below ordinary mode cutoff, very

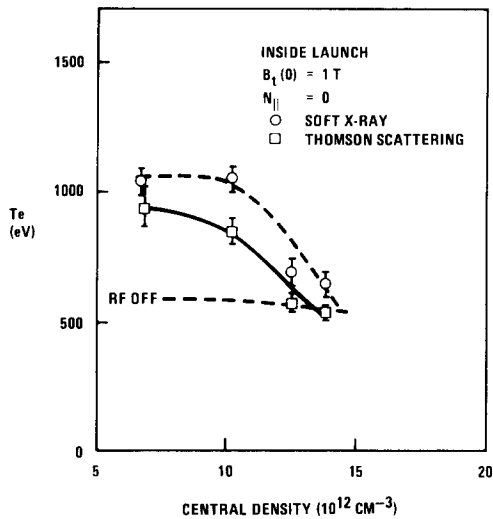


FIG. 3. Central heating as a function of density measured during the heating pulse for the perpendicular launch of the extraordinary mode with a central toroidal field of 1 T.

strongly attenuated the vertically polarized electric field component, while only partially attenuating (approximately 30%) the horizontal field component produced by the antenna.

For the perpendicularly propagating extraordinary mode, only the mode conversion damping process should be important, so that it might be expected that the observed heating would be a slowly varying function of density up to the central cutoff of  $2 \times 10^{13} \text{ cm}^{-3}$ . As can be seen from Fig. 3, which shows the central electron temperature as a function of density, the heating becomes negligible well before the predicted cutoff density is reached.

The behavior of heating as the magnetic field is varied may suggest the source of the difficulty. When the central toroidal field is reduced to 0.86 T, the central heating, shown in Fig. 4, is stronger and persists to a higher density even though the resonant surface has moved 12.6 cm inward of the minor axis. Moving the resonant surface outward from

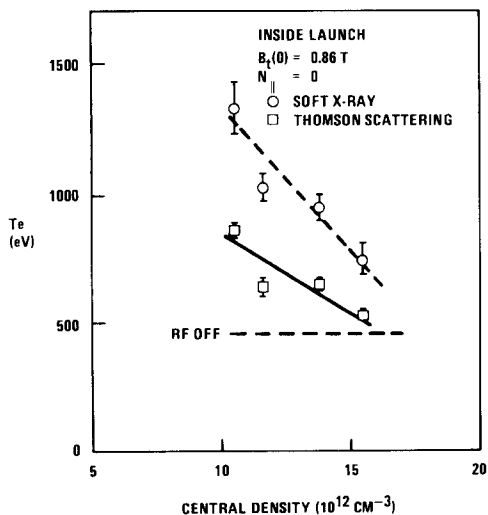


FIG. 4. Central heating as a function of density measured during the heating pulse for the perpendicular launch of the extraordinary mode with a central toroidal field of 0.86 T.

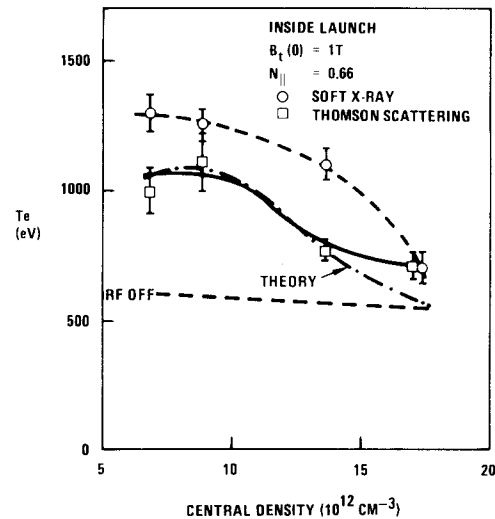


FIG. 5. Central heating as a function of density measured during the heating pulse for the oblique launch of the extraordinary mode with a central toroidal field of 1 T.

the center by a similar amount causes the central heating to essentially disappear. An important quantity associated with the damping that has such an asymmetry is the position of the upper hybrid resonant layer. Since the inverse of the damping process, used by cyclotron radiometers, does not show such a behavior, the asymmetry in the heating is probably due to a nonlinear effect. A possible candidate would be direct stochastic damping near the upper hybrid layer.<sup>11,12</sup> The asymmetry arises because as the toroidal magnetic field or the plasma density is increased, the upper hybrid layer moves into a lower temperature region nearer the edge. This results both in a higher local electric field and lower particle energy, both of which are conducive to nonlinear effects. If that is the correct explanation, then in larger tokamaks, in which the edge temperature is higher, the heating due to the mode conversion process may behave as expected from linear theory.

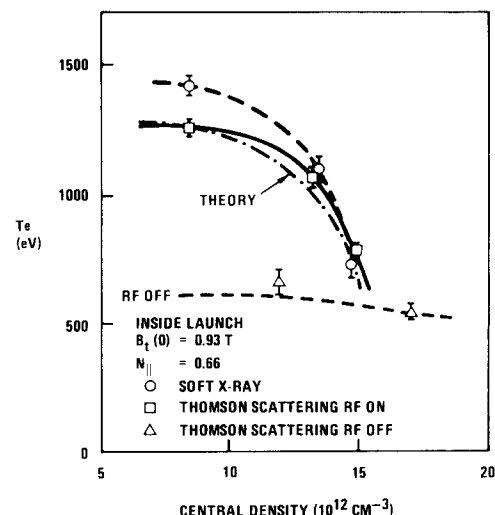


FIG. 6. Central heating as a function of density measured during the heating pulse for the oblique launch of the extraordinary mode for a central toroidal field of 0.93 T.

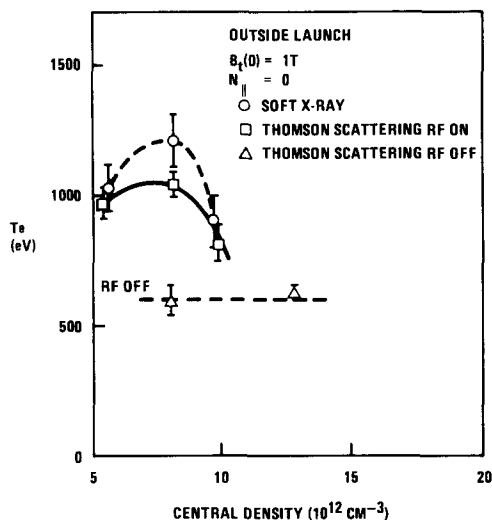


FIG. 7. Central heating as a function of density measured during the heating pulse for the perpendicular outside launch of the ordinary mode for a central toroidal field of 1 T.

For the more general case of an oblique launch angle, we were only able to make a rather sketchy exploration of the three-dimensional parameter space (angle, density, and magnetic field) in the time available to us. The results of that survey led us to concentrate most of our efforts on a launch angle of approximately  $42^\circ$  to the perpendicular ( $n_{\parallel} = 0.66$ ) which would be expected from the direct cyclotron damping theory to give strong single pass damping (52% at 600 eV and 80% at 1 keV at  $1 \times 10^{13} \text{ cm}^{-3}$  central density) and a cutoff density of  $1.6 \times 10^{13} \text{ cm}^{-3}$ . The data we obtained at that launch angle, which are given in Figs. 5 and 6, show greater central heating and higher density limit of heating than any other cases we examined.

In Figs. 5 and 6, the theoretical curve is obtained from a transport code calculation which self-consistently calculates the damping at each flux surface as a function of the local plasma parameters using only the direct cyclotron damping process. The heat deposition is then calculated and the plasma parameters recalculated, etc. The values of  $\tau_e$  and  $Z_{\text{eff}}$  are initially chosen to fit the Ohmic discharge data. The one turn voltage drop during heating is self-consistently calculated from the plasma parameters, while the density drop is externally imposed using the experimental data. The calculated one-turn voltage during heating, which does not include trapped particle effects, is within 10% of the measured value in the strongest heating case, and usually much closer. A more detailed description of the calculation can be obtained from Ref. 16.

For the case of a 1 T central field, shown in Fig. 5, the transport code calculation fits the Thomson scattering data for an incident microwave power of 80 kW, 64 kW of which is absorbed in the first pass, 80 kW agreeing well with our measured input power.

For the case of a 0.93 T central field shown in Fig. 6, the central heating is significantly stronger. In order to fit the Thomson scattering data for that case, the transport code calculation requires 80 kW absorbed and 100 kW incident, the latter exceeding our 80 kW input power. The greater

efficiency in the 0.93 T case may be due to a more effective contribution by the mode conversion process of that power (predicted to be 20% of the input) not damped in the first pass by the direct damping process, as suggested by the perpendicular launch observations. The code does not take such a contribution into account.

The localized nature of the power deposition by the extraordinary mode damping can be seen from a simple estimate of the heating efficiency in which it is assumed that the temperature and density profiles do not change shape, but the measured voltage drop and density drop are taken into account. The efficiency  $\eta$  is then given by

$$\eta = \left( \frac{\langle nT_e \rangle_{\text{rf}} \tau_{\Omega}}{\langle nT_e \rangle_{\Omega} \tau_{\text{rf}}} \right) \left( \frac{P_{\text{rf}} + P_{\Omega, \text{rf}}}{P_{\Omega}} \right)^{-1} \quad (2)$$

where  $\langle nT_e \rangle_{\Omega}$  and  $\langle nT_e \rangle_{\text{rf}}$  are the volume averaged energy before and 10 msec into the rf pulse, respectively,  $\tau_{\Omega}$  and  $\tau_{\text{rf}}$  are the respective electron energy confinement times, and  $P_{\Omega}$  and  $P_{\Omega, \text{rf}}$  are the respective Ohmic inputs. Assuming Al-cator scaling for  $\tau$ , then at the approximately  $9 \times 10^{12} \text{ cm}^{-3}$  density at which the heating was strongest, the apparent efficiency for the 1 T case was 116%, while that for the 0.93 T case was 140%. Most probably, this means that the profile narrowed or the energy was deposited in a narrower profile than the Ohmic deposition. The density reductions in these cases were slightly less than 30%, so there was a substantial net energy increase in both cases.

For the purpose of comparison, data from the outside launch experiments<sup>2</sup> are replotted in Fig. 7 using the same density scale as Figs. 3 through 6. (In the reference, the temperature data were plotted as a function of the initial density rather than the density at the time of the temperature measurement.) It is apparent that not only is the density cutoff more severe for the outside launch, but central heating is considerably poorer, especially when it is noted that the input power in this case was 110 kW. If again the profile is assumed unchanged by heating, the energy balance equation (2) gives an efficiency of 82% for this case. The predicted single pass damping for this case is approximately 50%.

#### IV. CONCLUSIONS

We have found that although at low densities (compared with the ordinary mode cutoff) any launch angle or polarization will produce significant heating, to obtain the best efficiency or heating to the highest possible density, some launching schemes are quite superior to others.

In particular, the obliquely launched extraordinary mode produced stronger central heating and heated to a higher density than the outside ordinary mode launch or the inside perpendicular extraordinary mode launch, the latter case showing a much more severe density limit than expected from theory. In contrast to the mode conversion process, the direct damping of the obliquely launched extraordinary mode works at least as well as theory predicts.

Based on that theory, at the higher initial temperatures of larger tokamaks, the density limit for the oblique extraordinary mode will approach twice the ordinary mode cutoff, because the value of  $n_{\parallel}$  required for strong direct damping is

smaller than in the present case. The predicted temperature and density dependence for direct damping of the extraordinary mode is also favorable for profile heating, because the lower density out on the profile partially compensates for the lower temperatures there, while for the ordinary mode, lowering either the temperature or density reduces damping.

## ACKNOWLEDGMENTS

We wish to acknowledge Dr. Yuji Tanaka for his management of the JFT-2 program, Dr. R. L. Freeman for his management of the General Atomic electron cyclotron heating program, Dr. N. Suzuki for the machine operation, Dr. H. Matsumoto for operation of the soft x-ray diagnostic, and Dr. T. Matoba for analysis of the Thomson scattering data. We would also like to thank Professor R. W. Gould for many useful suggestions concerning the microwave system.

This work was supported by the U.S. Department of Energy, Contract No. DE-AT03-76ET51011 and by the Japan Atomic Energy Research Institute.

<sup>1</sup>D. G. Bulyginsky, V. E. Golant, M. M. Larinov, L. S. Levin, and N. V.

Shustova, presented at the 2nd Joint Grenoble - Varenna International Symposium on Heating in Toroidal Plasmas, 3–12 September 1980.

<sup>2</sup>R. J. La Haye, C. P. Moeller, A. Funahashi, T. Yamamoto, K. Hoshino, N. Suzuki, S. M. Wolfe, P. C. Efthimion, H. Toyama, and T. Roh, Nucl. Fusion **21**, 1425 (1981).

<sup>3</sup>O. Eldridge, Phys. Fluids **15**, 676 (1972).

<sup>4</sup>A. L. Litvak, G. V. Permitin, E. V. Suvorov, and A. A. Frajman, Nucl. Fusion **17**, 659 (1977).

<sup>5</sup>I. Fidone, G. Granata, G. Rampani, and R. L. Meyer, Phys. Fluids **21**, 645 (1978).

<sup>6</sup>E. Ott, B. Hui, and K. R. Chu, Phys. Fluids **23**, 1031 (1980).

<sup>7</sup>T. H. Stix, Phys. Rev. Lett. **15**, 878 (1965).

<sup>8</sup>V. Kopecky, J. Preinhaelter, and J. Václavík, Plasma Phys. **3**, 179 (1969).

<sup>9</sup>J. Hosea, V. Arunasalam, and R. Cano, Phys. Rev. Lett. **15**, 408 (1977).

<sup>10</sup>V. S. Chan and S. C. Chiu, Phys. Fluids **25**, 683 (1982).

<sup>11</sup>A. T. Lin, C.-C. Lin, and J. M. Dawson, Phys. Rev. Lett. **47**, 48 (1981).

<sup>12</sup>S. E. Miller, Bell System Tech. J. **33**, 661 (1954).

<sup>13</sup>S. Silver, *Microwave Antenna Theory and Design* (McGraw-Hill, New York, 1949), p. 291.

<sup>14</sup>N. A. Krall and A. W. Trivelpiece, *Principles of Plasma Physics* (McGraw-Hill, New York 1973), p. 181.

<sup>15</sup>M. Gilgenbach, M. E. Read, K. E. Hackett, R. Lucey, B. Hui, V. L. Granatstein, K. R. Chu, A. C. England, C. M. Loring, O. C. Eldridge, H. C. Howe, A. G. Kulchar, E. Lazarus, M. Murakami, and J. B. Wilgen, Phys. Rev. Lett. **44**, 647 (1980).

<sup>16</sup>V. S. Chan, R. Davidson, G. Guest, M. Hacker, and R. L. Miller, presented at the 2nd Joint Grenoble-Varenna International Symposium on Heating in Toroidal Plasmas, 3–12 September 1980.